MINERALOGICAL MAGAZINE, DECEMBER 1971, VOL. 38, PP. 424–34

Chemical changes accompanying spherulitic crystallization in rhyolitic lavas, Central Volcanic Region, New Zealand

A. EWART
Department of Geology and Mineralogy, University of Queensland, St. Lucia, Queensland, 4067

SUMMARY. Spherulitic devitrification is a post-eruptive process affecting many rhyolitic lavas of the Taupo region. The spherulites consist of cryptocrystalline intergrowths of α-cristobalite and alkali feldspar (calcic anorthoclase), with minute granules of magnetite, hematite, and secondary (?)goethite. The effects of chemical fractionation occurring during progressive spherulite growth has been studied from a suite of samples from the Aratiatia rhyolite. The most significant effect is the progressive enrichment of both bulk spherulite compositions and the coexisting residual glass in potash with increasing spherulite development. This effect is due both to the very low potash in the earliest formed spherulites and to the consistently higher Na/K ratios of the spherulites relative to the total rock compositions. These differences progressively decrease with increasing spherulite crystallization. The bulk rock compositions, however, evidently remain essentially constant. The degree of potash enrichment in the residual glasses during advanced stages of devitrification is greater than expected by reference to the ternary feldspar and quartz–feldspar systems. This post-eruptive alkali fractionation during spherulite formation is superimposed on the pre-eruptive phenocryst–liquid fractionation.

IT is now well established that post-eruptive processes may significantly modify the chemistry of rhyolitic volcanic products. For example, alkali leaching (especially sodium loss) and oxidation of iron are likely during hydration of natural volcanic glasses (Lipman, 1965; Noble, 1967), and oxidation and halogen losses can be expected during devitrification (e.g. Noble, Smith, and Peck, 1967; Lipman, Christiansen, and van Alstine, 1968). Routine analyses of volcanic glasses separated from rhyolites of the Taupo region, New Zealand, also indicated that post-eruptive spherulite formation affected their compositions, resulting in pronounced potash enrichment in the glasses. A systematic study of one rhyolite extrusion, the Aratiatia rhyolite, was undertaken to study in detail the chemical effects of progressive spherulitic growth.

A detailed study of spherulitic crystallization in both welded tuffs and rhyolitic lavas from Japan was made by Tanida (1961). This account confirms and extends many of Tanida's results, using rocks of slightly differing composition and mineralogy. Similarly, Kesler and Weiblen (1968) have made detailed studies of chemical fractionation in andesitic spherulites, which showed different fractionation trends from the rhyolitic spherulites described in this paper. These authors also made estimates of their spherulite growth rates.

Petrography

The young rhyolitic lavas and domes of the Taupo region typically have an outer, vesicular glassy zone, frequently perlitic. This outer zone grades inwards to partly

spherulitic rock, which, by a gradual and irregular increase in the volume of spherulites, passes inwards into completely devitrified rock having no trace of residual volcanic glass. The rhyolitic lavas generally assume a spherulitic texture when devitrified, although this may be subsequently destroyed by continued recrystallization in the deeper parts of the larger flows.

The phenocrysts in the Taupo rhyolites are typically plagioclase (andesine), quartz, hypersthene, magnetite, ilmenite, less often calcic hornblende and biotite, and rarely sanidine. The occurrence of these phenocrysts has been previously discussed (Ewart, 1969).

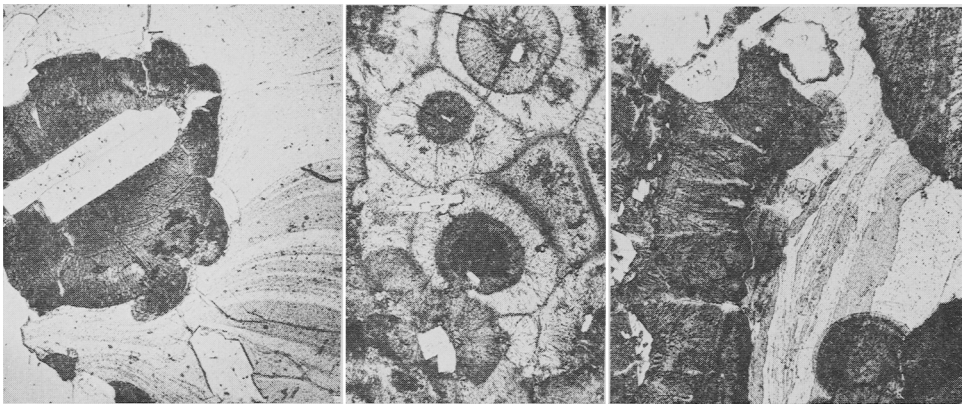

FIGS. 1 to 3: FIG. 1. (left). Spherulite (dark) with included plagioclase phenocryst. White phenocryst at bottom is also plagioclase. The flow lines within the residual glass matrix have been displaced around the phenocrysts, and then incorporated by the growing spherulite. Clear area at bottom left is edge of thin section. Total width of spherulite is 2·4 mm. Partly crossed nicols. Photo. S. N. Beatus. FIG. 2 (middle). Coalescing spherulites showing mutually polygonal outlines. Concentric zoning is visible in some of the spherulites. An interstitial microcrystalline (non-spherulitic) area (interpreted to be a devitrified residual glass area) is present in the middle right of the photograph. White phenocrysts are plagioclase. Total width of field of view 3 mm. Ordinary light. Photo. S. N. Beatus. FIG. 3 (right). Residual glass area showing flow lines, which are incorporated in, and pass undisturbed through, the adjacent spherulites. Smaller spherulites are visible growing on the margins of the larger ones. Plagioclase phenocryst at top left corner of photograph. Total width of field is 3·3 mm. Ordinary light. Photo. S. N. Beatus.

Spherulites. In the early stages of devitrification, spherulites occur mostly as isolated and nearly perfectly spherical bodies within the glass. They typically range from 1 to 5 mm in diameter, and in thin section exhibit both a radial-fibrous structure together with a concentric zoning made visible by slight changes of colour. The spherulites frequently appear to have nucleated on existing phenocrysts, especially plagioclase (fig. 1).

With increasing devitrification, the spherulites increase in number, coalescing in groups, thereby leaving isolated, irregular patches of residual glass. The coalesced spherulites frequently assume mutually polygonal outlines (fig. 2). The contacts between spherulites and residual glass are, however, often irregular due to the

occurrence of very small spherulites, which have seeded on the surfaces of larger ones (fig. 3).

In the final stages of devitrification, the residual interstitial glass areas become devitrified to microcrystalline, but non-spherulitic, aggregates within the otherwise spherulitic matrix (fig. 2).

Glass. The interstitial volcanic glass areas generally exhibit-well-defined flow structures, made visible by either orientation of crystallite rods, or by the alternation of narrow crystallite-rich and crystallite-poor zones (figs. 1 and 3). During progressive spherulitic development, the abundances of the crystallites appear to increase as the volume of residual glass decreases. A significant feature is the relationship between the flow structures within the glass relative to the adjacent spherulites; normally, the flow structures pass undisturbed through the spherulites (figs. 1 and 3), although in some examples slight deformation of flow structures is evident within or around a spherulite.

This evidence from the flow structures supports the views of, for example, Holmes (1920) and Morse, Warren, and Donnay (1932), that spherulitic crystallization occurs in lavas while in an extremely viscous to rigid state, and that crystallization is initiated rapidly following eruption.

Spherulite mineralogy

X-ray diffraction studies show the spherulites to be composed mainly of α-cristobalite and alkali feldspar (in cryptocrystalline intergrowths), as also found, for example, by Ross and Smith (1961) in devitrified welded tuffs. The feldspar peaks are broad and often ill-defined in the X-ray patterns. By reference to the data of Donnay and Donnay (1952), the feldspar can only be broadly classified as lying in the albite to anorthoclase compositional range. The presence of cristobalite and feldspar (and the absence of quartz) has been confirmed by infra-red absorption curves. The latter also show, in a qualitative way, the extremely disordered nature of the two phases. The feldspar absorption bands, for example, compare closely with those for alkali feldspar heated at 1050 °C for 28 to 30 days by Laves and Hafner (1962), and are much less sharp than those for soda and potash feldspars given by Lyon (1963).

Polished section examination reveals numerous minute irregular grains and strings of granules of iron oxides, often concentrated in concentric bands. The oxides are predominantly hematite, with marginal alteration to (?)goethite. In the centres of some of the larger grains, magnetite has been identified.

Chemical changes accompanying spherulitic crystallization

The Aratiatia Rhyolite has been described by Thompson (1966); it consists, in outcrop plan, of a set of concentric rhyolite dykes. Shallow drilling shows the rhyolite to be more extensive downwards. The rhyolite was temporarily well exposed during the excavations for the diversion tunnels, constructed as part of the Aratiatia hydro-electric station. From these exposures, a suite of samples was collected, representing the various stages of spherulitic devitrification.

Modal analyses of the samples are presented in table I, and chemical analyses of coexisting total rock, spherulite, and glass samples are presented in table II.

The analysed samples conform to the generalized mineralogical and petrographic outline previously given, except sample no. 7, which is texturally anomalous. This sample is completely devitrified; it consists, however, of two distinct textural phases, being partly spherulitic, but with extensive interstitial microcrystalline (non-spherulitic) areas. This type of texture appears to be more commonly found only in

TABLE I. *Modal analyses of the set of chemically analysed Aratiatia rhyolite lava specimens (based on 2000–2500 points)*

Sample*	No.	Phenocrysts†			Groundmass		
		Plagio-clase	Hyper-sthene	Magnetite	Spheru-litic	Glassy	Microcrystalline (non-spherulitic)
P. 34920	1	8·0	0·9	0·3	—	90·8	—
P. 34921	2	6·6	0·3	0·2	9·1	83·8	—
P. 34922	3	4·5	0·5	0·3	50·0	44·7	—
P. 34923	4	6·1	0·3	0·3	72·1	21·2	—
P. 34924	5	5·4	0·5	0·2	83·6	10·3	—
P. 34925	6	4·5	0·8	0·3	94·4	—	—
P. 34926	7	5·6	0·3	0·3	47·9	—	45·9

* New Zealand Geological Survey petrological collection numbers.
† No. 6 also has a very few hornblende phenocrysts.

the most advanced stages of spherulitic devitrification. The extensive microcrystalline areas are interpreted to represent original glass, coexisting with spherulites, which underwent subsequent devitrification after the cessation of the earlier spherulitic devitrification. The spherulitic crystallization in this case obviously ceased at an earlier stage of devitrification than is apparently normal.

Analytical methods. Relatively large total rock samples, weighing about 10 to 15 kg, were collected and coarsely crushed. Repeated quartering provided about 100 gms of sample for the total rock analyses. It proved necessary to make the initial separations of coexisting spherulites and glass by means of hand picking. The separates were then crushed to −230 mesh, washed, and all phenocryst material removed by conventional centrifuging techniques. The X-ray fluorescence techniques of Norrish and Chappell (1967) and Norrish and Hutton (1969) were finally used for all determinations, except sodium and ferric and ferrous iron. Sodium was determined by atomic absorption, and ferrous iron by the ammonium vanadate method (Wilson, 1955).

Results. The analytical data from table II, plotted in figs. 4 to 7, may be summarized:

The total rock compositions, with the exception of no. 1, are essentially similar within analytical uncertainty (excluding volatiles), as seen in the plots in figs. 4 and 5. The slightly greater spread of the points in fig. 4 can be attributed to the small variation of normative Q, resulting from oxidation of iron during progressive devitrification (fig. 7). No. 1 (which is vesicular and completely glassy) has a slightly lower Na_2O/K_2O

TABLE II. *Chemical analyses of total rocks and coexisting spherulites and residual glasses, separated from the Aratiatia rhyolite.* R, *total rock*; G, *glass*†; S, *spherulite*†; M, *microcrystalline (non-spherulitic) groundmass*†

	1R	1G	2R	2S	2G	3R	3S	3G	4R	4S	4G
SiO_2	72·48	74·56	74·06	77·44	76·84	74·91	78·77	76·83	74·97	77·69	75·95
Al_2O_3	12·63	12·00	12·89	12·72	12·32	12·87	12·14	12·44	13·00	12·33	12·19
TiO_2	0·23	0·15	0·23	0·16	0·16	0·23	0·16	0·16	0·23	0·15	0·15
FeO	1·04	0·80	1·45	0·87	1·17	1·24	0·80	1·16	0·97	0·74	1·16
Fe_2O_3	0·78	0·56	0·46	0·55	0·31	0·64	0·43	0·34	0·94	0·61	0·29
MnO	0·08	0·06	0·09	0·06	0·08	0·09	0·06	0·08	0·08	0·06	0·07
MgO	0·18	0·19	0·36	0·11	0·29	0·24	0·09	0·13	0·22	0·09	0·12
CaO	1·29	0·91	1·32	0·94	0·91	1·32	0·94	0·91	1·30	0·90	0·91
Na_2O	4·19	4·21	4·57	6·00	4·42	4·52	5·30	3·79	4·63	4·90	2·73
K_2O	3·10	3·13	2·86	0·75	3·21	2·83	1·28	4·25	2·70	2·31	5·77
P_2O_5	—	—	0·01	—	—	0·01	—	—	0·01	—	—
Ign.*	3·51	3·79	1·13	0·53	0·47	0·75	0·37	0·57	0·79	0·41	0·73
Total	99·51	100·36	99·43	100·13	100·18	99·65	100·34	100·66	99·84	100·19	100·07
Σ Fe as Fe_2O_3	1·94	1·45	2·07	1·52	1·61	2·02	1·32	1·63	2·02	1·42	1·58

	5R	5S	5G	6R	6S	7R	7S	7M
SiO_2	75·40	77·23	75·69	75·78	77·79	75·56	78·07	76·73
Al_2O_3	13·26	12·49	12·09	13·02	12·26	13·13	12·28	12·63
TiO_2	0·25	1·15	0·16	0·24	0·14	0·24	0·15	0·16
FeO	1·05	0·62	1·03	0·73	0·42	1·13	0·25	0·67
Fe_2O_3	0·94	0·65	0·45	1·20	0·85	0·71	0·55	0·75
MnO	0·09	0·07	0·08	0·07	0·06	0·08	0·02	0·05
MgO	0·26	0·13	0·23	0·22	0·14	0·25	0·04	0·14
CaO	1·31	0·96	0·87	1·30	0·85	1·27	1·03	0·88
Na_2O	4·53	4·66	2·93	4·52	4·37	4·63	4·89	4·06
K_2O	2·76	2·78	5·58	2·85	3·14	2·88	2·05	3·88
P_2O_5	—	—	—	—	—	—	—	—
Ign.*	0·55	0·41	0·45	0·40	0·34	0·27	0·26	0·10
Total	100·40	100·15	99·56	100·33	100·36	100·15	99·59	100·06
Σ Fe as Fe_2O_3	2·11	1·49	1·59	2·01	1·32	1·97	0·83	1·50

Analysts: A. Ewart (X-rays); Dr. R. Goguel (Na_2O).

* Ignition loss values of the spherulites and glasses are generally lower than the total rocks, due to drying procedures during mineral separations, resulting in some loss of $H_2O^{(-)}$.

† All spherulite and glass separates are phenocryst-free.

ratio. The ignition loss of this sample indicates a relatively high water content, and thus it is very possible that some sodium loss has occurred during hydration (Lipman, 1965; Noble, 1967).

The spherulites are enriched in Na_2O, SiO_2, and generally CaO, but depleted in K_2O, total iron, MgO, and MnO relative to their coexisting glasses. The spherulites also have lower ferrous/ferric ratios, there being some evidence that this ratio decreases with increasing spherulitic development (fig. 7). The glass from sample no. 1 apparently has an anomalously low ferrous/ferric ratio, but this may again be the result of hydration (Noble, 1967).

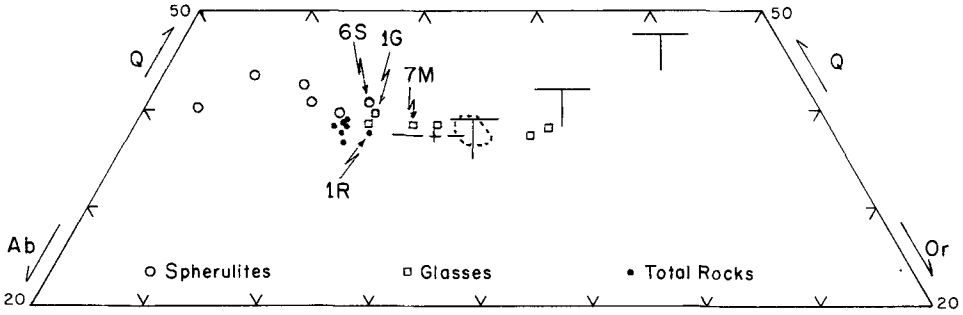

FIG. 4. Normative quartz, orthoclase, and albite compositions of the Aratiatia coexisting total rock, spherulite, and glass samples (table II) plotted in the Ab–Or–Q system. Numbers with letters refer to those in table II. The dashed area represents the compositional field of those groundmasses that coexist with phenocrystic quartz, plagioclase, and sanidine, separated from selected rhyolitic eruptive rocks of the Taupo region (after Ewart, 1969). The cross represents the minimum for 1 kilobar in the granite system (Tuttle and Bowen, 1958). The three piercing points are for 1 kilobar in the Ab–Or–An–Q–H_2O system, for compositions containing 3 %, 5 %, and 7·5 % An respectively (James and Hamilton, 1969).

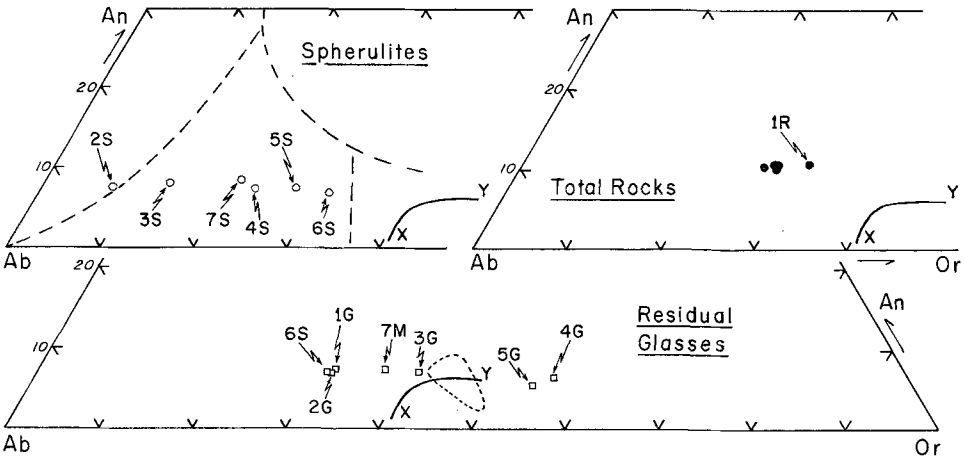

FIG. 5. Normative feldspar components of the Aratiatia coexisting total rock, spherulite, and glass samples (table II) plotted in the ternary diagrams Ab–Or–An. The numbers with letters refer to those in table II. The dashed area in the lower figure represents the compositional field of those groundmasses that coexist with phenocrystic quartz, plagioclase, and sanidine, separated from selected rhyolitic eruptive rocks of the Taupo region (after Ewart, 1969). The solid curved lines (marked *X–Y*) represent the projection of the two-feldspar surface with the silica surface (Carmichael, 1963). Limit of feldspar ternary solid solution and feldspar compositional limits (upper left diagram) after Smith and MacKenzie (1958).

The feldspar compositions of the spherulites (fig. 5) lie essentially within the anorthoclase field, and are thus broadly consistent with the X-ray diffraction data. Their high percentages of normative Q (37·03–40·46 %) are consistent with the very strong cristobalite reflections observed from the X-ray data. The spherulitic feldspar compositions are thus totally distinct from the phenocryst feldspars.

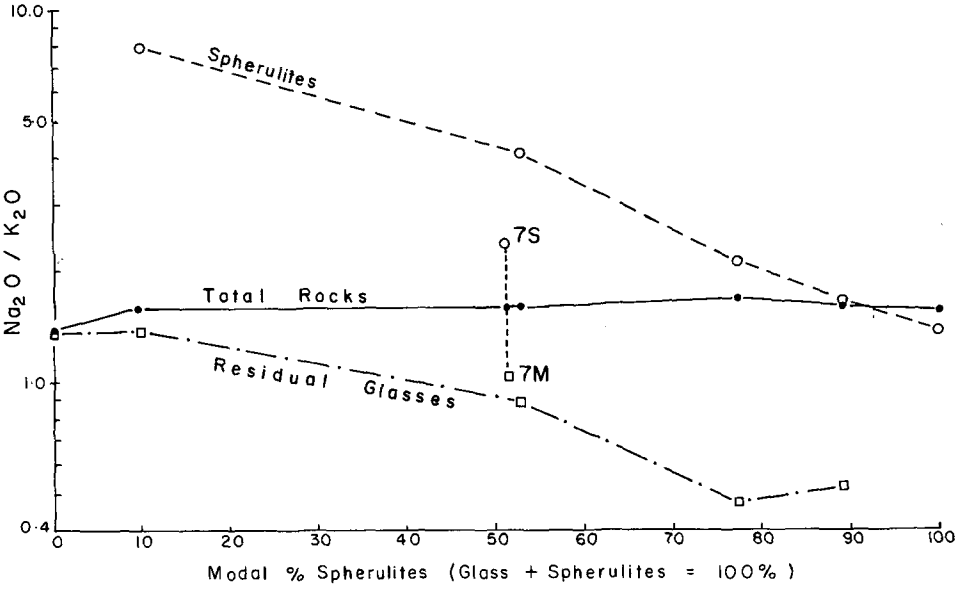

FIG. 6. Ratio Na_2O/K_2O versus modal % spherulites for the Aratiatia coexisting spherulites, residual glass, and total rock components (data from tables I and II).

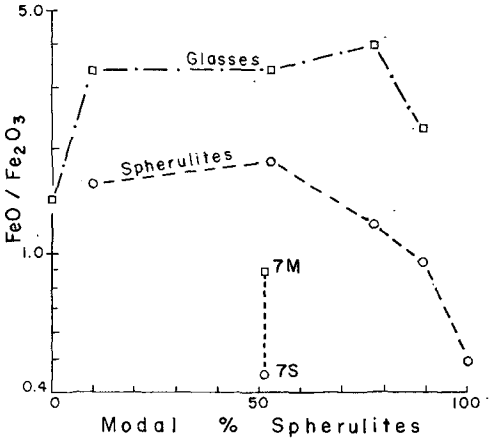

FIG. 7. Ratio FeO/Fe_2O_3 versus modal % spherulites for coexisting spherulites and residual glasses from Aratiatia.

It is evident from figs. 5 and 6 that both the spherulites and coexisting glasses exhibit a systematic variation in their alkali ratios with increasing spherulitic devitrification. In particular, fig. 6 indicates that the Na_2O/K_2O ratio of both phases continuously and simultaneously decreases with increasing spherulitic devitrification. Presumably, the change of bulk composition of the spherulites will be reflected in compositional

zoning (it has not been possible to check this by electron probe methods). This apparently anomalous effect arises from the fact that the spherulites are consistently enriched in sodium (with consequently higher Na/K ratios) relative to the total rock compositions, until spherulitic crystallization is nearly complete. These differences progressively decrease with increasing spherulite crystallization. Similar alkali fractionation effects between rhyolitic spherulites and their coexisting glass have been noted by other workers, e.g. Bryan (1954), Tanida (1961), and Simons (1962).

The spherulite and microcrystalline matrix data from sample no. 7 (= 7S and 7M) do not conform quantitatively to the fractionation patterns of the remaining spherulite–glass data (see especially fig. 6), for reasons not understood. This sample has already been noted as texturally anomalous. Nevertheless, even in this case the spherulites and microcrystalline matrix do exhibit the same overall trends of chemical fractionation as observed in the other spherulite–glass pairs.

Discussion

The alkali fractionation between spherulites and glass illustrated in figs. 4 to 6 is a post-eruptive effect, and is superimposed on the earlier (pre-eruptive) phenocryst–liquid fractionation. The liquid will be represented in the rocks in question by the total groundmass compositions (whether glassy, spherulitic, or partly spherulitic), unless modified by the devitrification processes.

In figs. 4 and 5, the various residual glass compositions are compared with the appropriate phase boundaries in the quartz–feldspar–water and ternary feldspar systems. It is clear that the trends delineated by the glass compositions during progressive potash enrichment show no particular tendency to coincide with the minimum or piercing points in fig. 4, or the two-feldspar boundary curve in fig. 5. This is emphasized by the fact that it has previously been shown (Ewart, 1969) that the compositions of those rare Taupo rhyolitic liquids (unmodified by post-eruptive processes) that coexist with phenocrystic quartz, plagioclase, and sanidine do show a close relationship to the appropriate phase boundaries in the ternary feldspar and quartz–feldspar systems. This is illustrated in figs. 4 and 5 by the dashed areas.

The conclusion reached, therefore, is that the degree of potash enrichment observed in the glasses during an advanced stage of spherulitic devitrification is greater than expected during normal phenocryst–liquid crystallization. Spherulitic crystallization is thus regarded as a quench phenomenon, and the observed chemical fractionation is evidently not controlled by the normal liquid–crystal equilibria. This is also suggested by the presence of cristobalite. As spherulitic crystallization is interpreted to occur in a very viscous or rigid lava state, the chemical changes observed imply extensive sub-solidus diffusion of the components. Nevertheless, as the total rock compositions remain essentially constant, the diffusion must evidently be localized and cannot involve any relatively large-scale alkali transfer.

The Aratiatia rhyolite does not contain phenocrystic sanidine or quartz and the compositions of both the total rock and its original residual liquid (represented by the total groundmass) must, therefore, lie within the primary plagioclase field of the quartz–feldspar and ternary feldspar systems. It is thus of some significance to

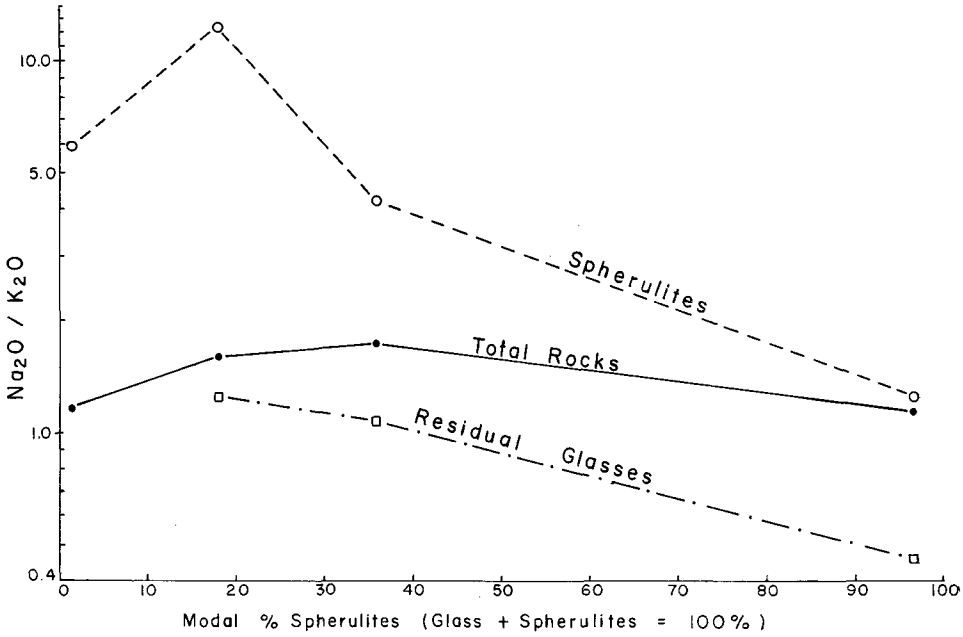

FIG. 8. Ratio Na_2O/K_2O versus modal % spherulites for coexisting spherulite, residual glass, and total rock components from other, randomly selected rhyolitic lavas of the Taupo region. Data from Ewart (1968, 1969) and table III.

TABLE III. *Previously unpublished analytical data used to construct fig. 8*

	P. 28361* Spherulites	P. 27575 Spherulites	P. 27574 Spherulites	P. 27854 Residual Glass	P. 27854 Spherulites
SiO_2	77·2	77·5	76·0	75·1	76·8
Al_2O_3	n.d.	12·4	n.d.	12·3	13·3
TiO_2	n.d.	0·06	n.d.	0·30	0·26
FeO	n.d.	0·9	n.d.	1·0	0·2
Fe_2O_3	n.d.	1·4	n.d.	0·35	0·6
MnO	n.d.	0·07	n.d.	0·05	0·02
MgO	n.d.	0·2	n.d.	0·3	0·15
CaO	1·3	0·95	1·4	0·9	0·8
Na_2O	4·7	6·15	5·70	2·7	4·3
K_2O	0·80	0·50	1·35	5·9	3·4
P_2O_5	n.d.	0·02	n.d.	0·02	0·02
H_2O^+	n.d.	0·34	n.d.	0·8	0·7
H_2O^-	n.d.	0·10	n.d.	0·2	0·1
Total		100·59		99·92	100·65

Analyst: J. A. Ritchie, Chemistry Division, N.Z.D.S.I.R.

* Sample numbers refer to the New Zealand Geological Survey petrological collection. Mineralogy and location of samples given in Ewart (1968).

compare the compositions of the completely glassy groundmass of sample no. 1 (= 1G in table II) and the completely spherulitic groundmass of sample no. 6 (= 6S in table II). Originally (i.e. before devitrification), these two groundmass compositions should have been practically identical. From figs. 4 and 5 it can be seen that in fact both groundmass compositions do plot very close together; the oxidation of iron during devitrification has resulted in a small relative increase in normative Q in 6S (fig. 4).

Alkali fractionation in other spherulitic rhyolites of the Taupo region

Fig. 8 has been constructed in order to try and ascertain whether the alkali fractionation during spherulitic growth, observed in the Aratiatia samples, is applicable to other rhyolitic lavas of the region. Fig. 8 is based on essentially randomly selected rhyolites, the basis of selection being simply the availability of analytical data on coexisting spherulite–glass–total rock compositions (table III). Compared to the similar plot in fig. 6, the trends in fig. 8 are more irregular, which is to be expected in view of both the variations in total-rock compositions and the variation in the extent of phenocryst crystallization between the different rhyolitic samples used. Nevertheless, it is apparent that the same type of chemical trends exist, and that the compositions of spherulites and coexisting residual glasses are evidently somewhat dependent on the extent of spherulitic devitrification.

Conclusions

Progressive post-eruptive spherulitic devitrification of rhyolitic lavas of the Taupo region results in a marked fractionation, especially of alkalis, between the spherulites and coexisting residual volcanic glass. Published data indicate that this is probably a common phenomenon in other rhyolites. In particular, enrichment of potassium in the glass during the advanced stages of devitrification is greater than occurs during normal (pre-eruption) crystal–liquid fractionation. Thus, any petrochemical study requiring the assessment of the bulk compositions of partly spherulitic rhyolitic groundmasses would have to be carefully undertaken. An example could be in the use of the recent plagioclase thermometer (Kudo and Weill, 1970). Similarly, sampling of partly spherulitic rhyolites would also have to be undertaken carefully in order to ensure that the samples were reasonably representative of the original bulk magma composition.

Acknowledgements. Considerable help was provided at an early stage of this investigation by R. A. Bailey, U.S. Geological Survey, which is gratefully acknowledged. S. Bagley provided a great deal of assistance in the X-ray fluorescence analyses.

REFERENCES

BRYAN (W. H.), 1954. *Proc. Roy. Soc. Queensland*, **65**, 51–69.
CARMICHAEL (I. S. E.), 1963. *Quart. Journ. Geol. Soc.* **119**, 95–131.
DONNAY (G.) and DONNAY (J. D. H.), 1952. *Amer. Journ. Sci. Bowen vol.* 115–32.
EWART (A.), 1968. *New Zealand Journ. Geol. Geophys.* **11**, 478–545.
—— 1969. *Lithos*, **2**, 371–88.

HOLMES (A.), 1920. *The Nomenclature of Petrology*. London (Thomas Murby & Co.).
JAMES (R. S.) and HAMILTON (D. L.), 1969. *Contr. Min. Petr.* **21**, 111–41.
KESLER (S. E.) and WEIBLEN (P. W.), 1968. *Amer. Min.* **53**, 2025–35.
KUDO (A. M.) and WEILL (D. F.), 1970. *Contr. Min. Petr.* **25**, 52–65.
LAVES (F.) and HAFNER (S.), 1962. *Norsk. Geol. Tidsskr.* **42**, 57–71.
LIPMAN (P. W.), 1965. *U.S. Geol. Surv. Bull.* **1201–D**, 24 pp.
—— CHRISTIANSEN (R. L.), and VAN ALSTINE (R. E.), 1968. *Amer. Min.* **54**, 286–91.
LYON (R. J. P.), 1963. *Evaluation of infrared spectrophotometry for compositional analysis of lunar and planetary soils*. Washington (N.A.S.A. Technical Note D–1871), 118 pp.
MORSE (H. W.), WARREN (C. H.), and DONNAY (J. D. H.), 1932. *Amer. Journ. Sci.* **23**, 421–39.
NOBLE (D. C.), 1967. *Amer. Min.* **52**, 280–6.
—— SMITH (V. C.), and PECK (L. C.), 1967. *Geochimica Acta*, **31**, 215–23.
NORRISH (K.) and CHAPPELL (B. W.), 1967. *In* ZUSSMAN (J.), (ed.), *Physical Methods in Determinative Mineralogy*, London and New York (Academic Press).
—— and HUTTON (J. T.), 1969. *Geochimica Acta*, **33**, 431–53.
ROSS (C. S.) and SMITH (R. L.), 1961. *U.S. Geol. Surv. Prof. Paper* **366**, 81 pp.
SIMONS (F. S.), 1962. *Amer. Min.* **47**, 871–85.
SMITH (J. V.) and MACKENZIE (W. S.), 1958. Ibid. **43**, 872–89.
TANIDA (K.), 1961. *Sci. Rep. Tohoku Univ.*, Ser. 3, 47–100.
THOMPSON (B. N.), 1966. *In* THOMPSON (B. N.), KERMODE (L. O.), and EWART (A.), (eds.), *New Zealand Volcanology, Central Volcanic Region*. N.Z. Dep. Sci. Industr. Res. Inf. Ser. No. 50, 73–4.
TUTTLE (O. F.) and BOWEN (N. L.), 1958. *Geol. Soc. Amer. Mem.* **74**, 153 pp.
WILSON (A. D.), 1955. *Bull. Geol. Surv. Gt. Britain*, **9**, 56–8.

[*Manuscript received 1 October 1970.*]